Nuclear Import of the Respiratory Syncytial Virus Matrix Protein Is Mediated By Importin β1 Independent of Importin α[†]

Reena Ghildyal,[§,#] Adeline Ho,[‡] Kylie M. Wagstaff,[‡] Manisha M. Dias,[‡] Chenoa L. Barton,[‡] Patricia Jans,[‡] Phillip Bardin,[#] and David A. Jans*[,‡,⊥]

Department of Biochemistry and Molecular Biology, Monash University, Clayton, Australia, Department of Microbiology, Monash University, Clayton, Australia, Department of Respiratory and Sleep Medicine, Monash Medical Centre, Clayton, Australia, and Australian Research Council Centre of Excellence for Biotechnology and Development, Australia

Received April 18, 2005; Revised Manuscript Received May 30, 2005

ABSTRACT: The matrix (M) protein of respiratory syncytial virus (RSV) plays an important role in virus assembly through specific interactions with RSV nucleocapsids and envelope glycoproteins in the cytoplasm as well as with the host cell membrane. We have previously shown that M localizes to the nucleus of infected cells at an early stage in the RSV infection cycle, where it may be instrumental in inhibiting host cell processes. The present study uses transient expression of M as well as a truncated green fluorescent protein (GFP) fusion derivative to show for the first time that M is able to localize in the nucleus in the absence of other RSV gene products, through the action of amino acids 110−183, encompassing the nucleic acid binding regions of the protein, that are sufficient to target GFP to the nucleus. Using native PAGE, ELISA-based binding assays, a novel Alphascreen assay, and an in vitro nuclear transport assay, we show that M is recognized directly by the importin β1 nuclear import receptor, which mediates its nuclear import in concert with the guanine nucleotide-binding protein Ran. Retention of M in the nucleus through binding to nuclear components, probably mediated by the putative zinc finger domain of M, also contributes to M nuclear accumulation. This is the first report of the importin binding and nuclear import properties of a gene product from a negative sense RNA virus, with implications for the function of RSV M and possibly other viral M proteins in the nucleus of infected cells.

Respiratory syncytial virus (RSV)[1] is the major viral cause of pneumonia and bronchiolitis in infants and is emerging as a major cause of pneumonia in the elderly. The RSV matrix (M) protein is a major structural protein of RSV, being essential for RSV replication and passaging (*1*). Although RSV is a cytoplasmic virus able to propagate in enucleated cells (*2*), the M protein of RSV localizes to the nucleus of infected cells early in infection (*3*). Intriguingly, the nuclei of RSV infected cells have been shown to be deficient in transcription, although this has yet to be demonstrated to be a direct effect of nuclear M.

The M proteins of other viruses within the *Paramyxoviridae* family such as Sendai virus and Newcastle disease virus (NDV) have also been shown to localize in the nucleus at early stages of virus infection (*4*, *5*). The M protein of vesicular stomatitis virus (VSV), which belongs to the related *Rhabdoviridae* family, has also been found to localize to the nucleus in infected cells (*6*), with both NDV and VSV M proteins having been shown to accumulate in the nucleus of transfected cells (*7*, *8*). Whereas nuclear targeting of NDV M is through a basic nuclear localization signal (NLS), two spatially separated regions appear to be responsible for nuclear localization of VSV M (*8*, *9*). VSV M has been shown to inhibit host cell transcription by inactivating essential transcription factors, thereby contributing to the "host-cell shutoff" observed in VSV-infected cells (*7*).

The pathway of nuclear import of RSV M and the other M proteins mentioned is not known. Proteins generally gain access to the nucleus through the action of NLSs that confer recognition by members of the importin (IMP) superfamily, which mediate translocation through the nuclear envelope (NE)-localized nuclear pore complexes (NPCs). In conventional nuclear protein import, such as that of the simian virus SV40 large tumor antigen (T-ag), the NLS is recognized by a heterodimeric complex of IMPα, which binds the NLS, and IMPβ1, which docks the transport complex at the NPC (*10*). The NLS substrate−IMP complex is then translocated through the NPC by a series of interactions with nucleoporins that line its central channel. Upon arrival at the nucleoplasmic

[†] The authors acknowledge the support of the National Health and Medical Research Council, Australia (Fellowship #143790/#333013 and Project Grant No. 143710 to D.A.J.).

* To whom correspondence should be addressed: Prof. David A. Jans, Department of Biochemistry and Molecular Biology, Monash University, Clayton, Vic 3800, Australia; tel: +613 9905 3778; fax: +613 9905 3726; e-mail: David.Jans@med.monash.edu.au

[‡] Department of Biochemistry and Molecular Biology, Monash University.

[§] Department of Microbiology, Monash University.

[#] Department of Respiratory and Sleep Medicine, Monash Medical Centre.

[⊥] Australian Research Council Centre of Excellence for Biotechnology and Development.

[1] Abbreviations: RSV, respiratory syncytial virus; M, matrix protein; NLS, nuclear localization signal; NPC, nuclear pore complex; NE, nuclear envelope; GFP, green fluorescent protein; IMP, importin; CLSM, confocal laser scanning microscopy; HA, influenza virus hemagglutinin epitope; T-ag, simian virus 40 large tumor antigen, VSV, vesicular stomatitis virus.

10.1021/bi050701e CCC: $30.25
Published on Web 08/30/2005

side of the NPC, the NLS-containing substrate−IMP complex is dissociated in the nucleus through binding of the monomeric guanine nucleotide-binding protein Ran in its GTP-bound form to IMPβ (*11*). Numerous nuclear import pathways have been described in which IMPα is not required, IMPβ1 or homologues thereof being sufficient to interact with the NLS-containing substrate as well as the NPC and Ran. IMPα-independent, IMPβ1-mediated nuclear import has been described for parathyroid hormone related protein (PTHrP), the sex determining region Y (SRY), T cell protein tyrosine phosphatase (TCPTP), yeast transcription factor GAL4, and telomere binding factor TRF-1 (*12*−*16*).

The present study examines RSV M nuclear import for the first time, showing that M is able to localize in the nucleus in the absence of other RSV gene products, through M amino acids 110−183, encompassing the previously described nucleic acid binding regions, which are sufficient to target green fluorescent protein (GFP) to the nucleus. Using a range of in vitro assays, we show that M is recognized directly by IMPβ1, independent of IMPα, and that it can mediate M nuclear import in concert with Ran. Retention of M in the nucleus through binding to nuclear components also contributes to M nuclear accumulation. This is the first report of the IMP binding and nuclear import properties of a protein from a negative sense RNA virus and has implications for the function of RSV M in the nucleus of infected cells.

MATERIALS AND METHODS

Construction of M Expression Clones. M gene was amplified from full-length RSV (A2 strain) cDNA (*17*) and cloned into the pET30a vector (Clontech) for expression as a hexa-His-tagged fusion protein in bacteria (His-M). The M gene was also subcloned into plasmid vector pSD4.2 (a gift from D. S. Lyles, Winston-Salem) in frame with the influenza HA epitope (M-HA). M amino acids 110−183 were cloned into the Gateway system as previously and fused in frame C-terminal to the GFP, for expression as a hexa-His-tagged GFP fusion protein in bacteria (pDESTGFPRfB vector (*18*), or as a simple GFP fusion protein in mammalian cells (pEPI-DESTC vector); the latter was generated from the episomally replicating GFP-fusion vector, pEPI-GFP (*19*) using the Invitrogen Gateway vector conversion system (Cat. No. 11828-029).

Protein Expression in Bacteria. With the exception of hexa-His tagged human (h) IMPβ1 which was purified under native conditions as previously reported, hexa-His-tagged-fusion proteins were expressed and purified under denaturing conditions (8 M urea) (*14*, *20*), followed by refolding on a NTA-affinity column and elution at 200 mM imidazole. Proteins were subsequently dialyzed, concentrated using a Centricon (30 000 MWCO), and stored in small aliquots at −70°C until use. Control molecules used were hexa-His-tagged GFP alone (*20*) and GFP-T-ag(111−135), containing the IMPα/β-recognized T-ag NLS (PKKKRKV^{132}) (*18*). Mouse (m) IMPα2 and β1 proteins used in binding experiments were expressed previously in bacteria as glutathione *S*-transferase (GST) fusion proteins and purified by affinity chromatography using glutathione sepharose (*21*, *22*). Truncated mouse IMPα2, lacking the first 69 amino acids and therefore in contrast to full-length IMPα able to bind IMPα/β-recognized NLSs with high affinity in the absence of IMPβ (*23*, *24*), was expressed and purified in identical fashion, as was GST alone.

Native Gel Electrophoresis. GFP-M(110−183), and His-M labeled with 5-iodoacetamino-fluorescein as previously reported (IAF-M) (*25*) were used in gel shift assays to determine interaction with IMPs. IAF-M or GFP-M or control GFP fusion proteins (5−25 pmol), with or without preincubation (15 min, room temperature) with IMPs (α, β1, or predimerized α/β1) at a final concentration of 0−12.5 μM in 25 μL, were loaded onto native polyacrylamide gels and electrophoresed at 80 V for 4−7 h at 4 °C. The position of the IAF-M or GFP fusion proteins in the gel were determined by fluorimaging using a Wallac Arthur 1422 Multiwavelength Fluorimager, with side illumination and exposure times of 0.25−2 s (*14*, *16*, *26*). In some cases, digital images were analyzed using the Image J 1.62 public domain software as previously used (*14*, *16*, *26*), where the fluorescence of the shifted band(s) was expressed as a fraction of the total fluorescence within the lane of the gel, after the subtraction of background fluorescence. Data were plotted and fitted for a sigmoidal function using the SigmaPlot 8.0 software.

ELISA-Based Binding Assay. An established ELISA-based assay (*21*, *22*, *25*, *27*, *28*) was used to determine the binding affinity of IMP subunits to RSV M protein. M protein was coated onto 96-well microtiter plates and incubated with increasing concentrations of IMP subunits, and bound IMP-GST was detected using an anti-GST primary antibody, an alkaline phosphatase-coupled secondary antibody, and the substrate *p*-nitrophenyl phosphate (*21*). Data were fitted as previously described to the function $B/B_{max} = [K_d + x + p - \sqrt{(-K_d - x - p)^2 - 4px}]/2p$, where x is the total concentration of probe (free + bound IMPs), B is the level of IMP bound, and p is the total concentration of protein, with the apparent dissociation constants (K_d) representing the IMP concentration yielding half-maximal binding (*16*).

In vitro Transport Assays. Nuclear import kinetics were measured at the single cell level using mechanically perforated HTC rat hepatoma cells in conjunction with confocal laser scanning microscopy (CLSM) as previously described (*14*, *22*). NLS-dependent nuclear protein import can be reconstituted in this system through the exogenous addition of cytosolic extract (untreated reticulocyte lysate-Promega Cat. No. L415A), an ATP regenerating system (0.125 mg/mL creatine kinase, 30 mM creatine-phosphate, 2 mM ATP), GTP (2 mM), and 70 kDa Texas Red-labeled dextran (Sigma Chemical Co.) to monitor nuclear integrity, and transport substrate (0.2 mg/mL IAF-labeled M). Where cytosolic extract was omitted, 45 mg/mL BSA was used, and where indicated, transport assays were also performed using reticulocyte lysate preincubated for 15 min at room temperature with anti-IMP antibodies (*29*). Some experiments were also performed in the presence of either the NE-permeabilizing agent CHAPS (0.025%), 300 μM GTPγS (nonhydrolyzable GTP analogue, Calbiochem) to block Ran activity, or 10 mM EDTA to assess the dependence on divalent cations. GFP-T-ag(111−135) (*18*) was used as a positive control. Image analysis of CLSM files using the Image J 1.62 software enabled determination of the nuclear-to-cytoplasmic ratio [Fn/c, the ratio of nuclear (Fn) to cytoplasmic (Fc) fluorescence, after the subtraction of fluorescence values due to

background/autofluorescence], with the results plotted and curve fitting performed using the Kaleidagraph 2.1 software to determine the nuclear transport kinetic parameters as previously described (*14*, *22*).

Expression of M in Mammalian Cells. M-HA was linearized with *Sal*1 and transcribed into mRNA using the SP6 mMessage mMachine transcription kit (Amicon). Vero cells were grown to 80% confluency in 35-mm Petri dishes and transfected with 2 μg of mRNA (M-HA) or plasmid DNA encoding GFP (pEGFP−C1) or GFP-M(110−183) mixed with 2 μL of lipofectamine in a total volume of 100 μL of Opti-MEM as per the manufacturer's recommendations (Invitrogen). Cells transfected with pEGFP−C1 or GFP-M(110−183) were imaged live by CLSM 24 h later. Cells transfected with M-HA were fixed with 4% formaldehyde, followed by permeabilization with 0.2% Triton X-100, and visualization of M-HA using rabbit polyclonal antibodies to HA (Sigma) and fluorescein-conjugated secondary antibodies and CLSM.

Alphascreen Assay. An Alphascreen (amplified luminescent proximity homogeneous assay) bead-based assay (Perkin-Elmer) was used to estimate the affinities of binding of biotin-labeled IMP-GSTs or GST alone (biotinylated using the Sulfo-NHS-Biotin reagent, according to the manufacturer's instructions, Pierce) to hexa-His-tagged M proteins. Binding of IMP to M brings the streptavidin-coated donor and Nickel-chelate-acceptor beads in sufficiently close proximity (200 nm) to enable transfer, upon photoactivation, of excited singlet oxygen from donor to acceptor bead to result in emission at 520−620 nm. Assays were performed in triplicate in an OptiPlate 384-well white opaque microtiterplate (Perkin-Elmer), whereby 30 nM hexa-His-tagged proteins were added to each well, followed by increasing amounts of IMP in PBS (137 mM NaCl, 6.25 mM Na_2HPO_4, 2.5 mM NaH_2PO_4) and incubated for 30 min at room temperature, after which 1 μL of a 1:10 dilution (in PBS) of the acceptor beads and 1 μL of 2.5% BSA were added and incubated for 90 min at room temperature. A total of 1 μL of a 1:10 dilution of the Donor beads was then added to give a final volume of 25 μL, and the mixture was incubated at room temperature for 2 h. The assay was then measured on a PerkinElmer FusionAlpha plate reader. Triplicate values were averaged, and the data were fitted to a sigmoidal function using SigmaPlot 8.0.

RESULTS

RSV M Is Recognized with High Affinity by IMPβ. As mentioned, RSV M protein localizes to the nucleus of cells early in infection (*3*). To assess whether M may enter the nucleus through a conventional IMP-dependent pathway, recombinant M was expressed in bacteria and purified, and IMP binding assessed using an established ELISA-based binding assay, previously used to determine binding affinities of various NLS-containing proteins (*22*, *29*). M was found to bind with high affinity to both mIMPβ1 (K_d of 14.6 ± 0.2 nM, $n = 2$) and the mIMPα/β heterodimer (K_d of 11.1 ± 1.2 nM, $n = 2$) but only with low affinity to mIMPα (K_d of 122 ± 21 nM, $n = 2$) (Figure 1). IMP binding to recombinant M labeled with IAF (IAF-M) was also assessed by native gel electrophoresis followed by fluorimaging, with IAF-M showing altered mobility in the presence of mIMPβ as well as the mIMPα/β heterodimer but not in the presence of mIMPα (data not shown). All results were consistent with the idea that nuclear import of M is likely to be mediated by IMPβ, independent of IMPα.

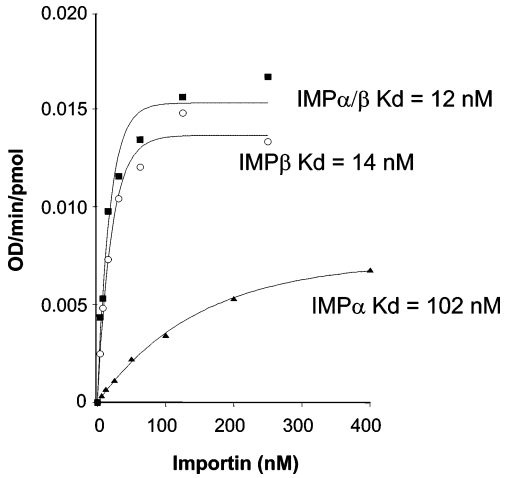

FIGURE 1: IMPβ but not IMPα interacts with RSV M with high affinity as determined using an ELISA-based binding assay. Microtiter plates were coated with His-M and incubated with increasing concentrations of recombinant GST-IMPs (α, β, or predimerized α/β complex). Bound IMPs were detected using an anti-GST primary antibody, an alkaline phosphatase-coupled secondary antibody, and the substrate *p*-nitrophenyl phosphate. Results are from a single experiment performed in triplicate representative of three separate experiments, with the apparent dissociation constants (K_d) for IMP/M binding indicated.

Nuclear Import of RSV M Is Dependent on IMPβ. To assess the ability of recombinant M to localize in the nucleus, M protein nuclear transport was examined in vitro using mechanically perforated HTC rat hepatoma cells; NLS-dependent nuclear protein import can be reconstituted in this system through the addition of exogenous cytosol and an ATP-regenerating system (*22*, *29*, *30*). IAF-M was found to accumulate strongly in the nuclei of perforated cells both in the presence and in the absence of cytosolic factors (Figure 2A) but to much higher levels (nuclear-to-cytoplasmic ratio (Fn/c) of ca. 20, representing 20-fold higher levels in the nucleus compared to the cytoplasm) in the presence of exogenous cytosol (Figure 2C), compared to in its absence (Fn/c of ca. 9, Figure 2D). Half-maximal accumulation was achieved within 6 min in the presence of cytosol. Clearly, maximal M nuclear import is dependent on cytosolic factors, although there is some nuclear accumulation of M in its absence, in part through M's ability to diffuse into the nucleus and accumulate by binding to nuclear components (see below).

As previously (*27*), dependence on IMPs was tested by adding specific anti-IMP antibodies to the in vitro transport system. Nuclear accumulation was reduced ca. 80% in the presence of anti-IMPβ1 antibodies, indicating the dependence of M nuclear import on IMPβ1; anti-IMPα antibodies, in contrast, slightly enhanced nuclear import (Figure 2AC). A similar trend was observed in the absence of cytosol (Figure 2AD), where nuclear accumulation was not affected by anti-IMPβ1 antibodies but was slightly enhanced by anti-IMPα antibodies; this may imply that residual IMPα remains in the system after the removal of cytosol, as we have previously shown in the case of IMPβ (*14*, *31*). Nuclear accumulation of the control molecule GFP-T-ag(111−135)

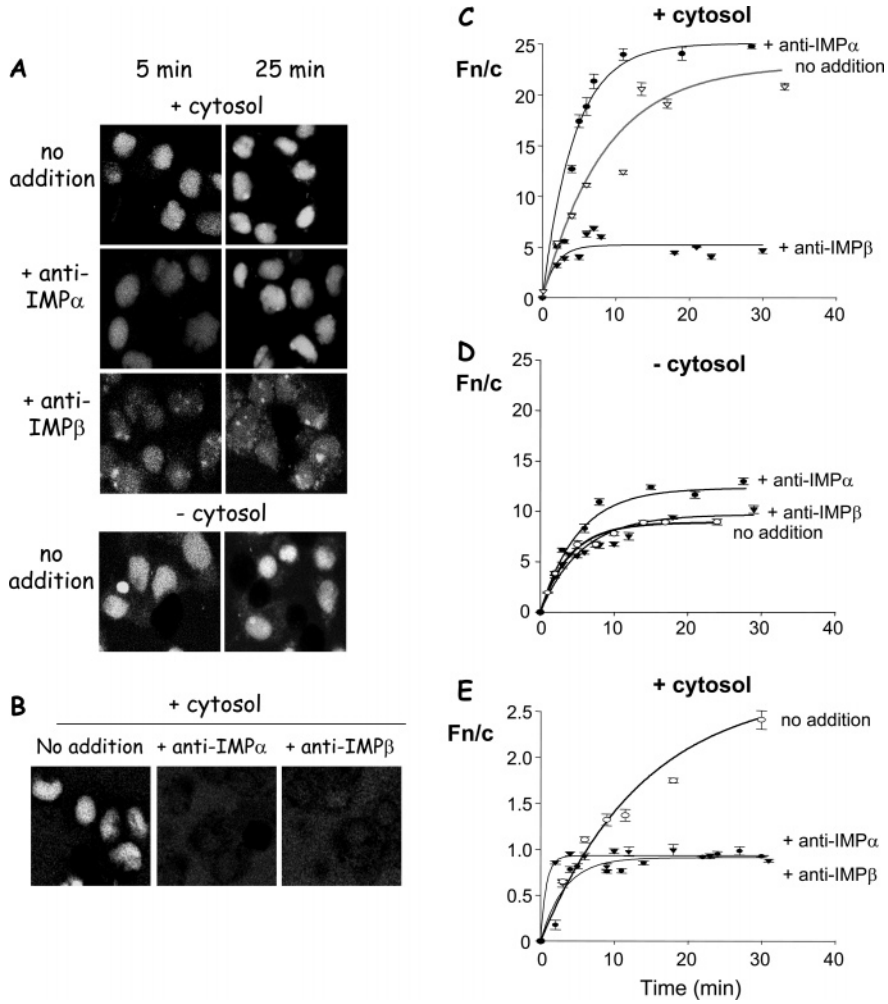

FIGURE 2: IMPβ mediates RSV M nuclear import. (A) Nuclear import of IAF-M was reconstituted in vitro in mechanically perforated HTC cells in the absence or the presence of exogenous cytosol, with or without (no addition) pretreatment with anti-IMP antibodies (40 μg/mL) in the presence of an ATP regenerating system. CLSM images were acquired at the indicated times for accumulation of IAF-M into intact nuclei. That the nuclei of the perforated cells were intact was shown by exclusion of 70 kDa Texas Red-labeled dextran (not shown). (B) Nuclear import for GFP-T-ag(111−135) was reconstituted as in panel A and CLSM images acquired after 25 min for accumulation of GFP-T-ag(111−135) in intact nuclei. (C) The nuclear import kinetics of IAF-M protein in the presence of exogenous cytosol in the absence or the presence of antibody to either IMPα or β was determined by image analysis of CLSM images such as those in panel A. Measurements shown are for the mean ± SEM from a single typical experiment, from a series of three separate experiments where each data point for the nuclear-to-cytoplasmic ratio (Fn/c) represents the mean of >12 separate measurements for each of Fn (nuclear fluorescence), Fc (cytoplasmic fluorescence), and background fluorescence. Data were fitted for the function $Fn/c = Fn/c_{max}\,(1 - e^{-kt})$, where Fn/c_{max} is the maximal level of nuclear accumulation, k is the rate constant, and t is the time in min. (D) Nuclear import kinetics of IAF-M protein in the absence of exogenous cytosol, in the absence or the presence of anti-IMP antibodies, analyzed as in panel C. (E) Nuclear import kinetics of GFP-T-ag(111−135) in the presence of cytosol and in the absence or presence of antibodies to IMPs, determined as in panel C.

was inhibited by both anti-IMPα and -IMPβ1 antibodies (Figure 2BE), demonstrating their functionality and that the effects on IAF-M were specific. In the absence of cytosol, anti-IMP antibodies had little or no effect on the nuclear accumulation of M (Figure 2D), consistent with the idea that M accumulates to a certain extent in the nucleus via diffusion/binding to nuclear components (see below). The transport data thus substantiated the gel shift and ELISA results, indicating the dependence of M nuclear import on IMPβ and lack of dependence on IMPα.

Nuclear Import of RSV M Is Dependent on Ran. The role of Ran in M nuclear import was tested by assessing the ability of the non-hydrolysable GTP analogue, GTPγS, to inhibit M nuclear accumulation in vitro. GTPγS reduced the maximal nuclear accumulation of IAF-M by ca. 60%, indicating the dependence of M nuclear import on Ran (Figure 3A). This was comparable to the effect (ca. 50% inhibition) on nuclear accumulation of the GFP-T-ag(111−135) (Figure 3C); that accumulation was not completely blocked by GTPγS is attributable in part to the fact that, like M, GFP-T-ag(111−135) is small enough to be able to enter the nucleus by passive diffusion (although in this case, there is no ability to accumulate by binding to nuclear factors; see below). As expected (Figure 3B), GTPγS had little effect on transport of IAF-M in the absence of cytosol. Taken together, the results presented in Figures 1−3 indicate that although there may be a contribution of diffusion/binding to nuclear components, maximal nuclear accumulation of M requires an active pathway dependent on IMPβ and Ran but not requiring IMPα; in fact, IMPα appeared to inhibit M nuclear import.

RSV M Binds to Nuclear Components. Nuclear accumulation of proteins can occur, in part, through nuclear retention via binding to DNA or nuclear-localized proteins, as has been

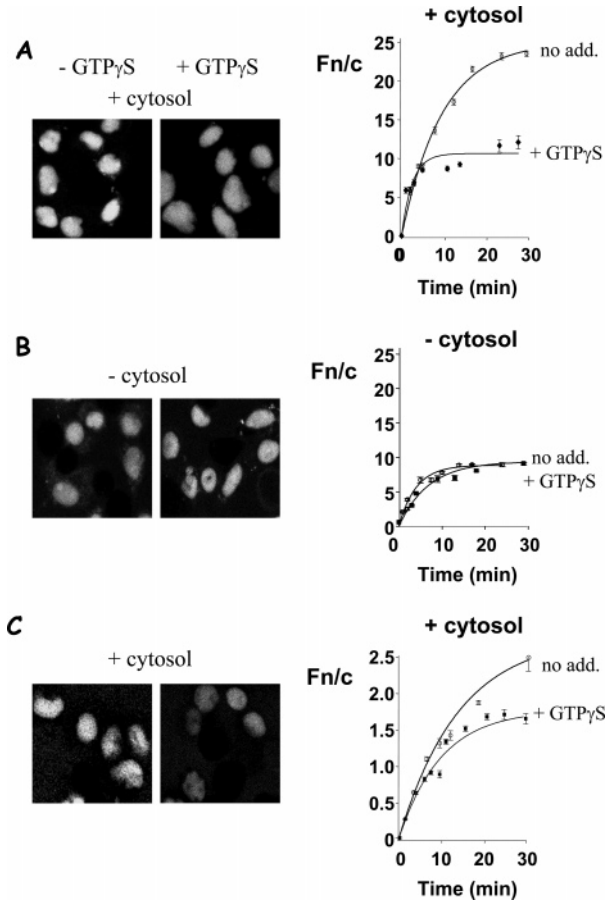

FIGURE 3: Nuclear import of M is inhibited by the nonhydrolyzable GTP analogue GTPγS. Nuclear import of IAF-M (A, B) or GFP-T-ag(111−135) (C) was reconstituted in vitro in mechanically perforated HTC cells in the presence (A, C) or absence (B) of exogenous cytosol, with or without the nonhydrolyzable GTP analogue GTPγS (300 μM). CLSM images acquired after 25 min are shown; that the nuclei of the perforated cells were intact was indicated by exclusion of 70 kDa Texas Red-labeled dextran (not shown). Quantitative analysis of CLSM images (rightmost panels) was performed as described in the legend to Figure 2.

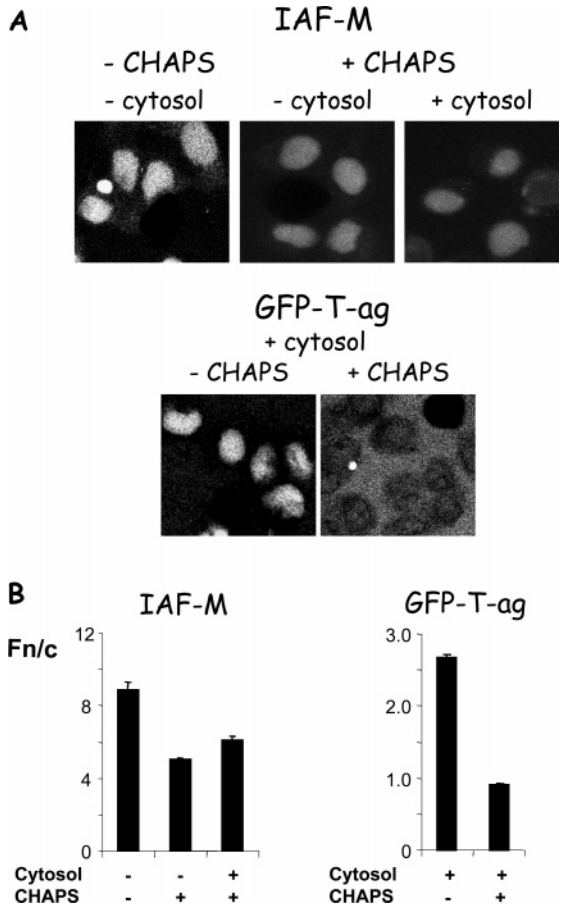

FIGURE 4: M is retained in the nucleus through interaction with nuclear components. Nuclear import of IAF-M and the control GFP-T-ag(111−135) molecule was reconstituted in vitro in mechanically perforated HTC cells in the absence or presence of 0.025% CHAPS and in the presence or absence of exogenous cytosol. (A) Visualization of nuclear uptake was performed using CLSM after 5 min at room temperature, with nuclear integrity monitored by exclusion of 70 kDa Texas Red-labeled dextran (not shown) in the absence, or entry thereof in the presence of CHAPS (as per Figure 5). (B) The Fn/c was quantitated as described in the legend to Figure 2.

shown for proteins such as the HIV-1 Tat protein (*27*) and the angiogenic factor angiogenin (*20*). To test for this possibility in the case of M, the NE-permeabilizing detergent CHAPS was used in the in vitro transport system; under these conditions, with no barrier to diffusion between nucleus and cytoplasm, proteins can only accumulate within the nucleus through binding to nuclear components (*27*). IAF-M was found to accumulate in the nucleus in the presence of CHAPS both in the presence and in the absence of exogenous cytosol (Figure 4AB) to levels ca. 6-fold those in the cytoplasm. Although the significance is not clear, we occasionally also observed accumulation of RSV M within the nucleolus of mechanically perforated HTC cells in the presence of CHAPS. This was in stark contrast to the GFP-T-ag(111−135), which, as shown previously (*27*), does not bind to nuclear components (Figure 4B) and fails to accumulate in the nucleus in the presence of CHAPS.

Metal Ion Chelator Inhibits RSV M Nuclear Accumulation and DNA Binding. M (aa 110−150) has been predicted to contain a zinc finger binding domain (ZFD) (*32*). To investigate the possibility that the M ZFD plays a role in nuclear accumulation/binding to nuclear components, transport experiments in the absence or presence of CHAPS were performed with or without short preincubation of M protein with 10 mM EDTA (Figure 5). Strikingly, EDTA significantly reduced nuclear accumulation over 50% in the absence of CHAPS, implying dependence of M nuclear accumulation on metal ions, most likely through the ZFD. This was in stark contrast to the control protein GFP-T-ag(111−135), which showed no inhibition of nuclear accumulation by EDTA treatment, in fact indicating a slight enhancement of nuclear import. Nuclear accumulation of IAF-M in the presence of CHAPS was also inhibited by EDTA treatment (Figure 5C, right panel). The implication was that metal chelation specifically inhibited nuclear import of M, presumably through preventing nuclear retention through the ZFD rather than through a general effect on the cellular nuclear transport machinery.

The RSV M Nuclear Targeting Sequence Resides within Amino Acids 110−183. As mentioned, RSV M protein localizes to the nucleus of infected cells early in infection (*3*). To confirm that this activity is intrinsic to M, and independent of other RSV components in the infected cell, transfection experiments were performed using RNA encoding HA-tagged M (Figure 6B, left panel). Immunostaining of the fixed cells followed by image analysis clearly

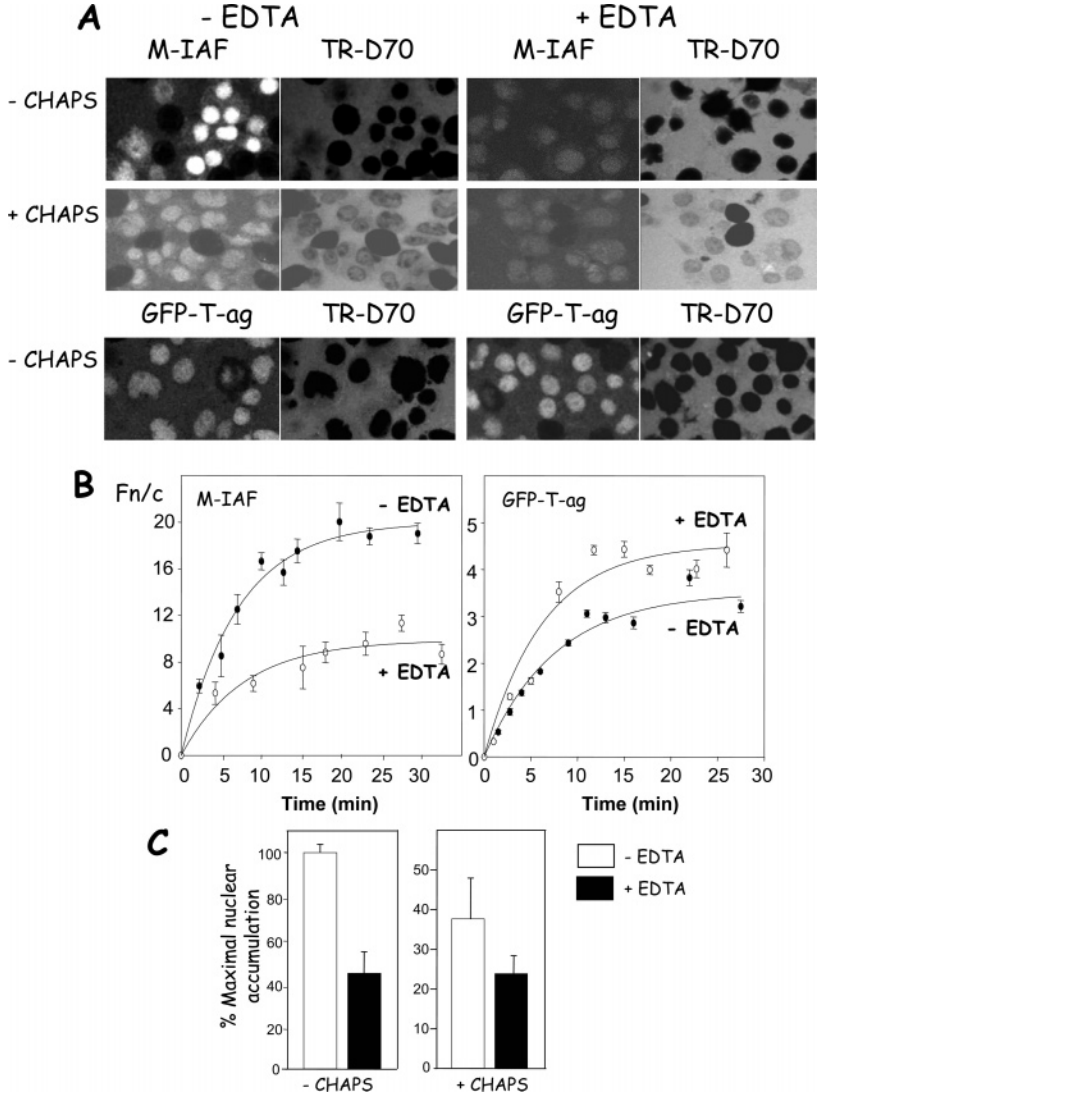

FIGURE 5: M nuclear accumulation in the absence or presence of CHAPS is inhibited by the metal chelator EDTA. Nuclear import of IAF-M and the control GFP-T-ag(111−135) molecule was reconstituted in vitro in mechanically perforated HTC cells in the presence of exogenous cytosol, in the absence or the presence of 0.025% CHAPS, as described in the legend to Figure 4. (A) Visualization of nuclear uptake was performed using CLSM after 5 min at room temperature (A), with nuclear integrity monitored by exclusion of 70 kDa Texas Red-labeled dextran (TR-D70) in the absence or entry thereof in the presence of CHAPS as indicated. (B, C) Nuclear (Fn/c) accumulation was quantitated as described in the legend to Figure 2C; the data in panel C are presented as a percentage of maximal accumulation of IAF-M in the absence of CHAPS.

demonstrated M's ability to localize in the nucleus in the absence of other RSV components (Figure 6B, left panel).

In addition to the putative ZFD implicated as being important for RSV M's ability to accumulate in the nucleus in vitro (see above), its central domain contains two sequences (amino acids 120−130 and 154−172) believed to be responsible for nucleic acid binding (see Figure 6A). As a first step toward mapping the location of the sequences within RSV M responsible for recognition by IMPβ1 and nuclear import, we generated a mammalian cell expression construct expressing M amino acids 110−183 fused to GFP. Figure 6B shows that M residues 110−183 alter the localization of GFP from diffusely throughout the cell (middle panel) to predominantly nuclear (right panel) (change in Fn/c from 1 to 2.4), implying that these residues contain the NLS of M.

To test whether this region is responsible for IMPβ interaction, a hexa-His-tagged GFP-M(110−183) derivative was expressed in bacteria and purified for use in in vitro binding experiments (Figure 6C), results from native gel electrophoresis/fluorimaging indicating recognition of GFP-M(110−183), but not of GFP alone, by both mIMPβ and hIMPβ, in a fashion similar to full-length M (compare to Figure 1). GFP-M(110−183) also bound to mIMPα/β, in a fashion similar to full-length M (Figure 1). M amino acids 110−183 thus represent the residues within M responsible for IMPβ binding. That binding by mIMPβ and hIMPβ yielded different electorphoretic mobilities in the native gels is attributable to the fact that the m and hIMPs are GST- and hexa-His-tagged fusions, respectively. Native gel electrophoresis/fluorimaging was also used (not shown) to determine that IMPβ residues 2−485 are responsible for binding RSV M amino acids 110−183.

A modified amplified luminescent proximity homogeneous assay (Alphascreen) (manuscript in preparation) was used to compare the binding affinities for His-M and GFP-M(110−183) of biotinylated mIMPβ-GST and a "nonauto-inhibited" truncated form of mIMPα (TrIMPα)-GST, able

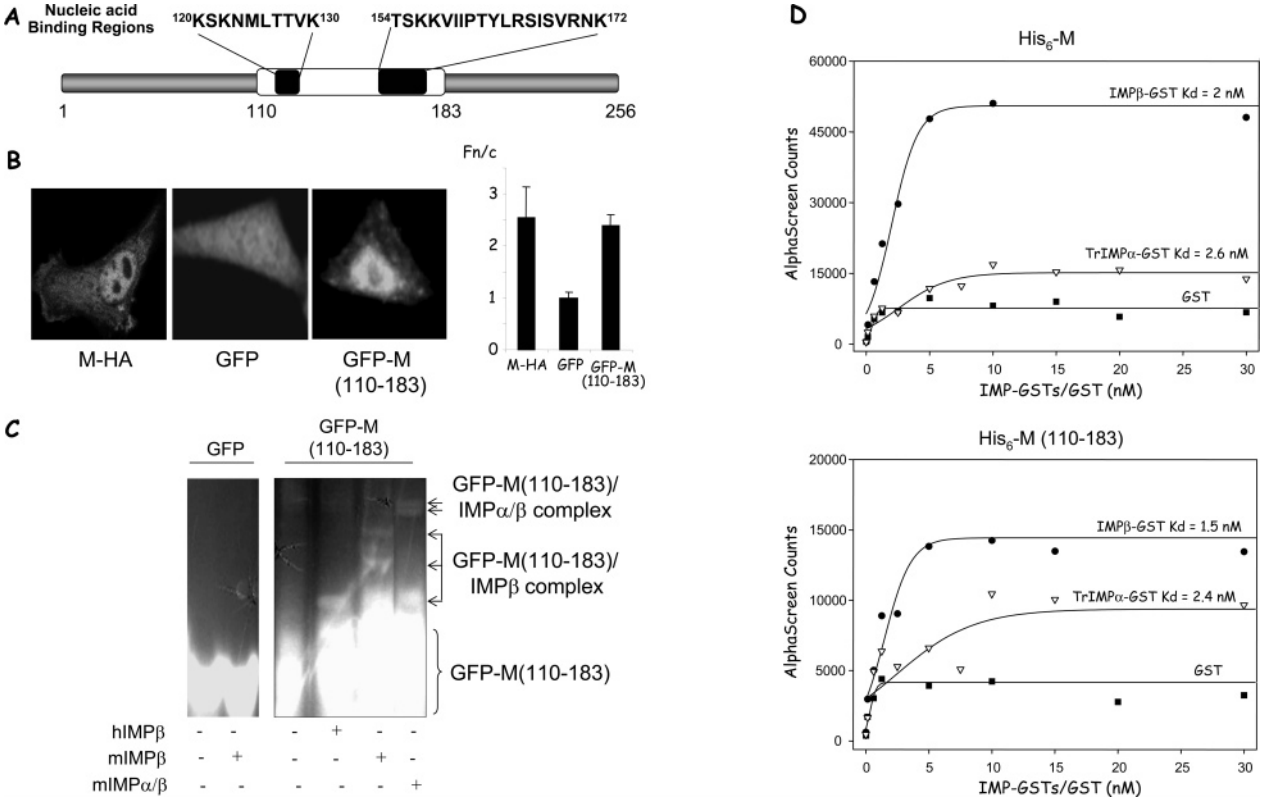

FIGURE 6: M amino acids 110−183 mediate nuclear localization and IMPβ binding. (A) Schematic diagram of M protein showing the nucleic acid binding regions (black) and the region (white box), including the putative ZFD (amino acids 110−150) contained within GFP-M(110−183). Numbers refer to the residue numbers in the M sequence. (B) Vero cells were transfected to express full-length M with a HA fusion tag (left panel), GFP (middle panel), or GFP-M(110−183) (right panel). Subcellular localization of M-HA was visualized 8 h after transfection by immunofluorescence and CLSM as described in Materials and Methods. GFP and GFP-M(110−183) localization was visualized by CLSM of live cells 24 h after transfection. Image analysis was performed on the CLSM images as described in the legend to Figure 2C. The results represent the mean ± SEM ($n \geq 10$). (C) 5 μM bacterially expressed GFP-M(110−183) was incubated with 10 μM GST tagged mouse or hexa-His-tagged human IMPβ1 (mIMPβ or hIMPβ, respectively) or predimerized mIMPα/β1 for 15 min at room temperature prior to native PAGE and fluorimaging. The positions of GFP-M(110−183) and complexes with IMPs are indicated. (D) Alphascreen assay. His-M or hexa-His-GFP-M(110−183) were incubated with increasing concentrations of biotinylated IMPα- or IMPβ-GST, or GST itself as a control, and an Alphascreen bead-based assay, performed as described in Material and Methods, used to determine the affinity of binding. Sigmoidal curve fitting (regression coefficients ≥ 0.984) was performed using the SigmaPlot software, with the calculated K_d's indicated; results are from a single experiment performed in triplicate representative of 2−3 separate experiments.

to bind IMPα/β-recognized NLSs with high affinity in the absence of IMPβ (*23*, *24*). As indicated in Figure 6D, the binding properties of His-M and GFP-M(110−183) were essentially identical, IMPβ binding to a markedly higher extent (>3-fold), and with greater affinity (K_d of 1.4 ± 0.7 nM, $n = 3$, and 1.4 ± 0.6 nM, $n = 2$ for full-length and M110−183, respectively) than TrIMPα. That the GST moiety did not influence binding significantly was indicated by the fact that biotinylated GST alone did not markedly bind either M protein (Figure 6D). Results confirmed that M amino acids 110−183, additional to being sufficient to target GFP to the nucleus, contained the IMPβ binding site within M.

DISCUSSION

The present study represents the first delineation of the nuclear import pathway of a paramyxovirus M protein and also the first for a gene product from a negative sense RNA virus. We have shown that the RSV M protein residues 110−183 are sufficient to mediate nuclear localization of GFP via a pathway dependent on IMPβ1 and Ran but not IMPα. Additionally, we have shown that interaction with nuclear components may contribute to M accumulation in the nucleus. Thus, M utilizes an IMPβ1-dependent nuclear import pathway distinct from that of T-ag, which uses an IMPα/β-dependent classical pathway, but comparable to that of PTHrP, TRF1, and HIV-1 Rev (*12*, *13*, *16*, *33*). Indeed, the nuclear import pathway of PTHrP resembles that of M very closely (*13*); both PTHrP and M are small enough to diffuse through the NPC and accumulate to some extent in the absence of cytosolic factors through binding to nuclear/nucleolar components, but efficient nuclear accumulation in both cases requires active transport dependent on IMPβ and Ran. Our preliminary analysis in the case of RSV M (Figure 5 and unpublished results) indicates that M may potentially be retained in the nucleus through binding to DNA sequences, dependent on its ZFD, but this needs to be confirmed using various other approaches.

The various IMP binding experiments show that M is capable of associating with both IMPβ and IMPα/β, the latter probably being mediated through IMPβ, as IMPα itself, and a truncated, nonautoinhibited derivative thereof, are unable to bind M with high affinity (Figures 1 and 6D, and data not shown). Antibodies to IMPβ but not IMPα impair M nuclear accumulation in vitro, while the nonhydrolyzable GTP analogue GTPγS inhibits M nuclear import, demonstrating the dependence of M nuclear import on IMPβ and Ran. Interestingly, antibodies to IMPα enhanced M nuclear

import to a certain extent, implying that IMPα inhibits M nuclear import, which has previously been observed for the IMP*β*-recognized PTHrP and TRF1 nuclear import cargoes (*13*, *16*). Since the IMPα/*β* heterodimer can clearly bind M as shown here, this inhibition does not appear to be due to competition for binding sites on IMP*β* but perhaps indicates that the M−IMPα/*β* complex is not "productive" for nuclear import, as has been reported for various IMPα/*β*-recognized but not import cargoes such as histone H1 and ribosomal protein rpL23a (*34*, *35*). A "nonproductive" interaction of M with IMPα/*β* would be expected to inhibit M nuclear import and would explain the enhancement of M nuclear import by antibodies to IMPα.

Our results here show for the first time that M residues 110−183 are sufficient to target GFP to the nucleus and bind to IMP*β* with high (nanomolar) affinity. Intriguingly, M residues 110−183 appear to possess nucleic acid (*36*) binding activity, which could potentially mask the NLS activity in a fashion analogous to the transcription factors GAL4 (*12*) and SRY (*14*, *26*), where binding to specific DNA sequences competes with IMP*β*1 binding and nuclear import; similar mechanisms apply to the TATA-binding protein and its nuclear import receptor Kap114p (*37*). Recent work has shown that at later stages of infection, M is predominantly in the cytoplasm associated with nucleocapsids (*38*) and can bind to the viral RNA (*39*). An attractive possibility is thus that M interaction with viral RNA in the nucleocapsids may mask its NLS, thus inhibiting nuclear import. Alternatively, DNA binding by M in the nucleus, possibly to inhibit transcription of specific host cell genes (*3*), could mask its NLS and facilitate export from the nucleus. The precise significance of RSV M-DNA binding in the infected cell context, e.g., whether it relates to binding to specific gene promoters or chromatin sites, etc., remains to be examined in detail, but interesting possibilities in this regard are that, in a fashion analogous to VSV M (*40*, *41*), it may play a role in suppressing transcription of genes such as *β*-interferon to reduce antiviral responses.

Intriguingly, our results show that EDTA is able to inhibit M nuclear accumulation in either the absence or the presence of an intact nuclear envelope (Figure 5), implying that the main target of the action of the metal chelator is M's nuclear retention, possibly mediated through DNA binding, consistent with our preliminary observations (data not shown) showing that M amino acids 110−183 may mediate DNA binding in the absence but not the presence of EDTA. In contrast, EDTA increased nuclear accumulation of a GFP-T-ag protein (Figure 5). While further experimentation, beyond the scope of this study, is clearly necessary to assist in determining the mechanism, an intriguing possibility is that the effects may relate to the findings of Schweizer and Hanover (*42*), who found that high levels of Ca^{2+} inhibited Ran activity in an in vitro nuclear transport system. Since Ca^{2+} ions are present in the intracellular buffer used in our in vitro system, it is not inconceivable that Ran activity may be inhibited to some extent, such that EDTA can overcome the inhibition to lead to slightly increased nuclear accumulation. The extent to which EDTA may generally enhance nuclear import in in vitro systems is currently under investigation in this laboratory.

As the first study investigating the mechanism of nuclear transport of a gene product from a negative sense RNA virus, our report has far-ranging implications. Since paramyxovirus replication occurs entirely within the cytoplasm, it seems clear that the concerted nuclear targeting of a viral protein is likely to be required to achieve a specific effect on host cell nuclear processes such as transcription/RNA splicing/ribosome assembly. The M proteins of various negative sense viruses have indeed been implicated in causing the cytopathic effects associated with infection, with VSV M, for example, shown to be involved in the inhibition of host cell transcription and in causing the characteristic cell rounding observed in VSV-infected cells (*40*, *41*). Insight into RSV M's functions in the nucleus, whether through DNA/RNA binding, or some other mechanism, will be crucial to understanding pathogenesis mediated by RSV and the role therein of M. Importantly, it may also assist in identifying new targets to enable the future development of urgently needed anti-RSV therapeutics.

ACKNOWLEDGMENT

The authors acknowledge the support of the National Health and Medical Research Council, Australia (Fellowship #143790/#333013 and Project Grant No. 143710 to D.A.J.). Thanks are due to Khairil Latiff for construction of the M-HA clone and to Tracy Waterhouse for cell culture.

REFERENCES

1. Teng, M. N., and Collins, P. L. (1998) Identification of the respiratory syncytial virus proteins required for formation and passage of helper-dependent infectious particles. *J. Virol. 72*, 5707−5716.
2. Follett, E. A., Pringle, C. R., and Pennington, T. H. (1975) Virus development in enucleate cells: echovirus, poliovirus, pseudorabies virus, reovirus, respiratory syncytial virus and Semliki Forest virus. *J. Gen. Virol. 26*, 183−196.
3. Ghildyal, R., Baulch-Brown, C., Mills, J., and Meanger, J. (2003) The matrix protein of Human respiratory syncytial virus localises to the nucleus of infected cells and inhibits transcription. *Arch. Virol. 148*, 1419−1429.
4. Peeples, M. E., Wang, C., Gupta, K. C., and Coleman, N. (1992) Nuclear entry and nucleolar localization of the Newcastle disease virus (NDV) matrix protein occur early in infection and do not require other NDV proteins. *J. Virol. 66*, 3263−3269.
5. Yoshida, T., Y., N., Yoshii, S., Maeno, K., and Matsumoto, T. (1976) Membrane (M) protein of HVJ (Sendai virus): its role in virus assembly. *Virology 71*, 143−161.
6. Lyles, D. S., Puddington, L., and McCreedy, B. J. J. (1988) Vesicular stomatitis virus M protein in the nuclei of infected cells. *J. Virol. 62*, 4387−4392.
7. Ahmed, M., and Lyles, D. S. (1998) Effect of vesicular stomatitis virus matrix protein on transcription directed by host RNA polymerases I, II, and III. *J. Virol. 72*, 8413−8419.
8. Coleman, N. A., and Peeples, M. E. (1993) The matrix protein of Newcastle disease virus localizes to the nucleus via a bipartite nuclear localization signal. *Virology 195*, 596−607.
9. Glodowski, D. R., Petersen, J. M., and Dahlberg, J. E. (2002) Complex nuclear localization signals in the matrix protein of vesicular stomatitis virus. *J. Biol. Chem. 277*, 46864−46870.
10. Bayliss, R., Littlewood, T., and Stewart, M. (2000) Structural basis for the interaction between FxFG nucleoporin repeats and importin-beta in nuclear trafficking. *Cell 102*, 99−108.
11. Englmeier, L., Olivo, J. C., and Mattaj, I. W. (1999) Receptor-mediated substrate translocation through the nuclear pore complex without nucleotide triphosphate hydrolysis. *Curr. Biol. 9*, 30−41.
12. Chan, C. K., Hubner, S., Hu, W., and Jans, D. A. (1998) Mutual exclusivity of DNA binding and nuclear localization signal recognition by the yeast transcription factor GAL4: implications for nonviral DNA delivery. *Gene Ther. 5*, 1204−1212.
13. Lam, M. H., Briggs, L. J., Hu, W., Martin, T. J., Gillespie, M. T., and Jans, D. A. (1999) Importin beta recognizes parathyroid

hormone-related protein with high affinity and mediates its nuclear import in the absence of importin alpha. *J. Biol. Chem. 274*, 7391−7398.
14. Forwood, J. K., Harley, V., and Jans, D. A. (2001) The C-terminal nuclear localization signal of the sex-determining region Y (SRY) high mobility group domain mediates nuclear import through importin beta 1. *J. Biol. Chem. 276*, 46575−46582.
15. Tiganis, T., Flint, A. J., Adam, S. A., and Tonks, N. K. (1997) Association of the T-cell protein tyrosine phosphatase with nuclear import factor p97. *J. Biol. Chem. 272*, 21548−21557.
16. Forwood, J. K., and Jans, D. A. (2002) Nuclear import pathway of the telomere elongation suppressor TRF1: inhibition by importin alpha. *Biochemistry 41*, 9333−9340.
17. Jin, H., Clarke, D., Zhou, H. Z., Cheng, X., Coelingh, K., Bryant, M., and Li, S. (1998) Recombinant human respiratory syncytial virus (RSV) from cDNA and construction of subgroup A and B chimeric RSV. *Virology 251*, 206−214.
18. Baliga, B. C., Colussi, P. A., Read, S. H., Dias, M. M., Jans, D. A., and Kumar, S. (2003) Role of prodomain in importin-mediated nuclear localization and activation of caspase-2. *J. Biol. Chem. 278*, 4899−4905.
19. Piechaczek, C., Fetzer, C., Baiker, A., Bode, J., and Lipps, H. J. (1999) A vector based on the SV40 origin of replication and chromosomal S/MARs replicates episomally in CHO cells. *Nucleic Acids Res 27*, 426−428.
20. Lixin, R., Efthymiadis, A., Henderson, B., and Jans, D. A. (2001) Novel properties of the nucleolar targeting signal of human angiogenin. *Biochem. Biophys. Res. Commun. 284*, 185−193.
21. Hubner, S., Xiao, C. Y., and Jans, D. A. (1997) The protein kinase CK2 site (Ser111/112) enhances recognition of the simian virus 40 large T-antigen nuclear localization sequence by importin. *J. Biol. Chem. 272*, 17191−17195.
22. Hu, W., and Jans, D. A. (1999) Efficiency of importin alpha/beta-mediated nuclear localization sequence recognition and nuclear import. Differential role of NTF2. *J. Biol. Chem. 274*, 15820−15827.
23. Fontes, M. R., Teh, T., Jans, D., Brinkworth, R. I., and Kobe, B. (2003) Structural basis for the specificity of bipartite nuclear localization sequence binding by importin-alpha. *J. Biol. Chem. 278*, 27981−27987.
24. Kobe, B. (1999) Autoinhibition by an internal nuclear localization signal revealed by the crystal structure of mammalian importin alpha. *Nat. Struct. Biol. 6*, 388−397.
25. Efthymiadis, A., Shao, H., Hubner, S., and Jans, D. A. (1997) Kinetic characterization of the human retinoblastoma protein bipartite nuclear localization sequence (NLS) in vivo and in vitro. A comparison with the SV40 large T-antigen NLS. *J. Biol. Chem. 272*, 22134−22139.
26. Forwood, J. K., Lam, M. H., and Jans, D. A. (2001) Nuclear import of Creb and AP-1 transcription factors requires importin-beta 1 and Ran but is independent of importin-alpha. *Biochemistry 40*, 5208−5217.
27. Efthymiadis, A., Briggs, L. J., and Jans, D. A. (1998) The HIV-1 Tat nuclear localization sequence confers novel nuclear import properties. *J. Biol. Chem. 273*, 1623−1628.
28. Xiao, C. Y., Hubner, S., and Jans, D. A. (1997) SV40 large tumor antigen nuclear import is regulated by the double-stranded DNA-dependent protein kinase site (serine 120) flanking the nuclear localization sequence. *J. Biol. Chem. 272*, 22191−22198.
29. Hubner, S., Smith, H. M., Hu, W., Chan, C. K., Rihs, H. P., Paschal, B. M., Raikhel, N. V., and Jans, D. A. (1999) Plant importin alpha binds nuclear localization sequences with high affinity and can mediate nuclear import independent of importin beta. *J. Biol. Chem. 274*, 22610−22617.
30. Jans, D. A., Ackermann, M. J., Bischoff, J. R., Beach, D. H., and Peters, R. (1991) p34cdc2-mediated phosphorylation at T124 inhibits nuclear import of SV-40 T antigen proteins. *J. Cell Biol. 115*, 1203−1212.
31. Schedlich, L. J., Le Page, S. L., Firth, S. M., Briggs, L. J., Jans, D. A., and Baxter, R. C. (2000) Nuclear import of insulin-like growth factor-binding protein-3 and -5 is mediated by the importin beta subunit. *J. Biol. Chem. 275*, 23462−23470.
32. Latiff, K., Meanger, J., Mills, J., and Ghildyal, R. (2004) Sequence and structure relatedness of matrix protein of human respiratory syncytial virus with matrix proteins of other negative-sense RNA viruses. *Clin. Microbiol. Infect. 10*, 945−948.
33. Henderson, B. R., and Percipalle, P. (1997) Interactions between HIV Rev and nuclear import and export factors: the Rev nuclear localisation signal mediates specific binding to human importin-beta. *J. Mol. Biol. 274*, 693−707.
34. Bauerle, M., Doenecke, D., and Albig, W. (2002) The requirement of H1 histones for a heterodimeric nuclear import receptor. *J. Biol. Chem. 277*, 32480−32489.
35. Jakel, S., and Gorlich, D. (1998) Importin beta, transportin, RanBP5 and RanBP7 mediate nuclear import of ribosomal proteins in mammalian cells. *EMBO J. 17*, 4491−4502.
36. LaCasse, E. C., and Lefebvre, Y. A. (1995) Nuclear localization signals overlap DNA- or RNA-binding domains in nucleic acid-binding proteins. *Nucleic Acids Res. 23*, 1647−1656.
37. Pemberton, L. F., Rosenblum, J. S., and Blobel, G. (1999) Nuclear import of the TATA-binding protein: mediation by the karyopherin Kap114p and a possible mechanism for intranuclear targeting. *J. Cell Biol. 145*, 1407−1417.
38. Ghildyal, R., Mills, J., Murray, M., Vardaxis, N., and Meanger, J. (2002) The respiratory syncytial virus (RSV) matrix protein associates with nucleocapsids in infected cells. *J. Gen. Virol. 83*, 753−757.
39. Rodriguez, L., Cuesta, I., Asenjo, A., and Villanueva, N. (2004) Human respiratory syncytial virus matrix protein is an RNA-binding protein: binding properties, location and identity of the RNA contact residues. *J. Gen. Virol. 85*, 709−719.
40. Lyles, D. S., and McKenzie, M. O. (1997) Activity of vesicular stomatitis virus M protein mutants in cell rounding is correlated with the ability to inhibit host gene expression and is not correlated with virus assembly function. *Virology 229*, 77−89.
41. Kopecky, S. A., Willingham, M. C., and Lyles, D. S. (2001) Matrix protein and another viral component contribute to induction of apoptosis in cells infected with vesicular stomatitis virus. *J. Virol. 75*, 12169−12181.
42. Sweitzer, T. D., and Hanover, J. A. (1996) Calmodulin activates nuclear protein import: a link between signal transduction and nuclear transport. *Proc. Natl. Acad. Sci. U.S.A. 93*, 14574−14579.

BI050701E